*The 2014 World Congress on*
***Advances in Civil, Environmental, and Materials Research (ACEM14)***
*Busan, Korea, August 24-28, 2014*

# Effect of porosity and permeability reduction on hydrate production in marine sediments

*Ah-Ram Kim[1)]and Gye-Chun Cho[2)]

[1), 2)] *Department of Civil Engineering, KAIST, Daejeon 305-600, Korea*
[2)] gyechun@kaist.ac.kr

## ABSTRACT

Methane hydrate production by depressurization in marine sediments, which consist of sand or mud layers, induces pore pressure decrease, effective stress increase, and, simultaneously, porosity reduction. The permeability of the sediments then drops around the production well and the depressurized range and hydrate dissociation range are affected by the porosity and permeability reduction. In this study, a field scale simulation using the finite difference method (FDM) was conducted to investigate not only the effects of porosity and permeability reduction but also the geomechanical responses of hydrate-bearing sediments during methane production. Moreover, the coupled mechanical-flow-thermal model incorporates latent heat,thermal conduction, and thermal advection due to pore fluid flow to more closely simulate the physical processes in marine sediments.

## 1. INTRODUCTION

Methane hydrate is an ice-like solid compound in which methane molecules are locked within lattice structures of water. Hydrate-bearing sediment, which is found in offshore and permafrost regions, is anticipated to exist in 113 regions according to geophysical, geochemical, and geological investigations (Kvenvolden and Lorenson 2010). During the past 30 years, research has been used to make a global estimation of methane gas in hydrate-bearing sediments ofabout $10^{15}$ $m^3$ STP (Milkov 2004). Currently fourteen main hydrate productionprojects are underway around the world (Boswell and Collett 2010).

There are three main methods of gas recovery from methane hydrate layers: (1) depressurization, in which the methane hydrate is dissociated by lowering the well pressure; (2) thermal stimulation, in which the hydrate is dissociated by injecting hot fluid into the production well; and (3) chemical stimulation, in which the hydrate is destabilized by injecting inhibitors and their combinations (Moridis 2003; Makogon 1997;

---

[1)]Graduate Student
[2)]Professor

Holder et al. 1984; Pawar et al. 2005). For successful methane recovery from hydrate deposits, depressurization is considered the most productive and effective method (Moridis and Reagan 2007; Collett 2007).

This study focuses on the effects of porosity reduction which is induced by depressurization during methane gas production, and on the geomechanical responses of hydrate-bearing sediments during the production period. Two-dimensional axisymmetric numerical modeling is conducted using a finite difference method FLAC2D (Itasca 2005) to simulate field-scale methane production from the Ulleung basin by depressurization. Moreover, the coupled mechanical-hydraulic-thermal model incorporates pore fluid flow, hydrate dissociation, effective stress increment, and thermal effect (e.g. latent heat,thermal conduction, and thermal advection) to more closely simulate the physical processes in marine sediments.

## 2. DESCRIPTION OF SITE

The potential for methane hydrate deposits to exist in the Ulleung Basin, located at the southwestern corner of the Korean East Sea, was suggested by the Korea Institute of Geoscience and Mineral Resources (KIGAM) between 2000 and 2004 (Park 2006). The basin has a water depth of 2157 m; the depth of the hydrate occurrence zone is 140-153 mbsf (Fig. 1a).

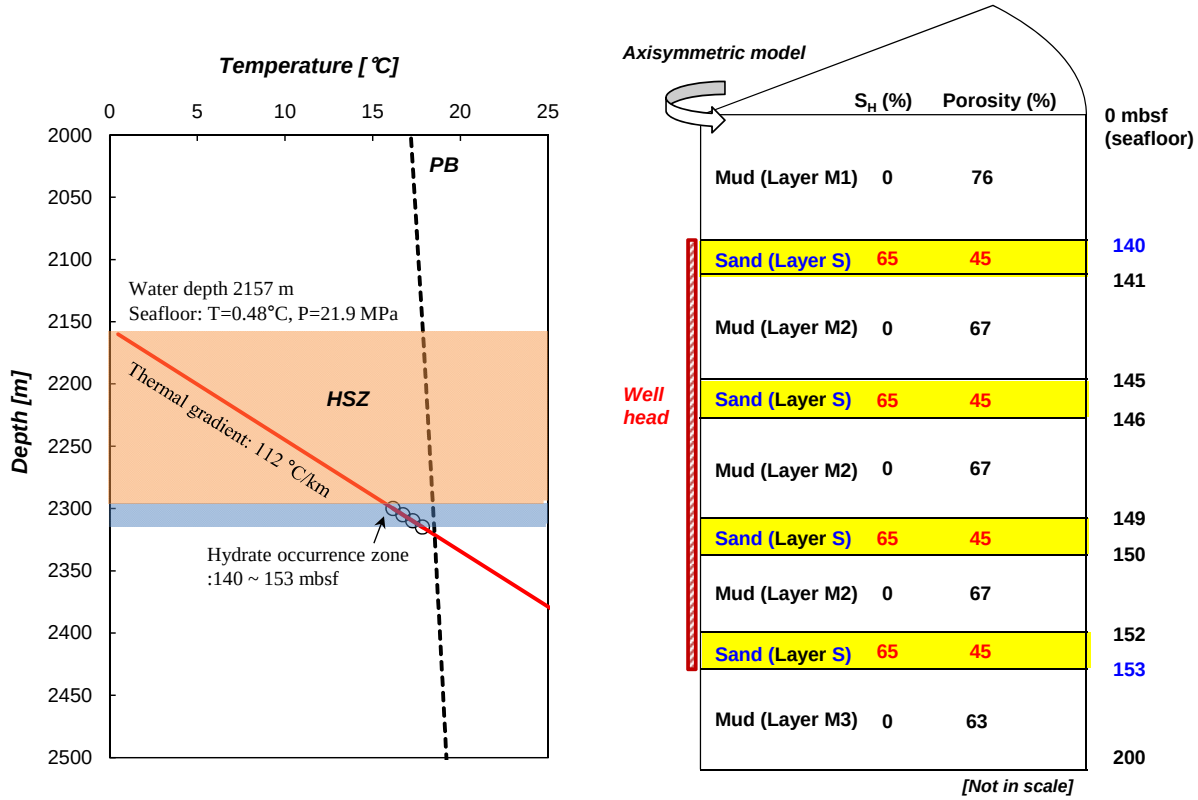


Fig.1 Geological and environmental conditions: (a) hydrate occurrence zone and hydrate stability zone (HSZ) (b) geometry of UBGH2-6B in the Ulleung basin

Based on core samples and logging data (Ryu et al. 2012), the study site has been found to consist of non-hydrate mud layers and sand layers one meter in length in the hydrate occurrence zone. The initial hydrate saturation in the sand layers was found to be 65% (Fig. 1b). A sediment deposit 200 m deep and 200 m wide was modeled as an axisymmetric mesh. The well head, which uses a vertical line type of pressure stimulation, is positioned at the left boundary (i.e., 140-153 mbsf). As a comparative study, two depressurization scenarioswere set up to decrease monotonically from the initial pore pressure to 5 MPa, and 9 MPa.

Table 1. Geologic conditions used in this study

| Properties | Values |
|---|---|
| Hydrostatic pressure at seafloor [MPa] | 21.9 |
| Temperature at seafloor [°C] | 0.482 |
| Geothermal gradient [°C $km^{-1}$] | 112 |
| Hydrate occurrence zone [mbsf] | 140-153 |
| Initial hydrate saturation in sand (Layer S) [%] | 65 |
| Initial hydrate saturation in mud (Layer M1, M2, M3) [%] | 0.0 |
| Hydrate number, $N_h$ | 6 |
| Salinity [wt%] | 3.5 |

Table 2.Mechanical properties used in this study

| Properties | Values |
|---|---|
| Bulk density of sand (Layer S) [kg $m^{-3}$] | 1700 |
| Bulk density of Mud (Layer M1) [kg $m^{-3}$] | 1500 |
| Bulk density of Mud (Layer M2) [kg $m^{-3}$] | 1610 |
| Bulk density of Mud (Layer M3) [kg $m^{-3}$] | 1640 |
| Density of seawater [kg $m^{-3}$] | 1035 |
| Methane hydrate density [kg $m^{-3}$] | 910 |
| Porosity of sand (Layer S) [ - ] | 0.45 |
| Porosity of mud (Layer M1) [ - ] | 0.76 |
| Porosity of mud (Layer M2) [ - ] | 0.67 |
| Porosity of mud (Layer M3) [ - ] | 0.63 |
| Bulk modulus of water [GPa] | 2 |

Table 1 shows the detailed geologic conditions and parameters of the study site as used in the simulation. The phase boundary is determined by considering the water depth (i.e., 2157 m), the geothermal condition of formation (i.e., a temperature at the seafloor of 0.482°C and a geothermal gradient of 112 °C/km), and the seawater salinity (i.e., 3.5 wt%). The intrinsic permeability and the mechanical properties (Table 2) used here were determined from the results of laboratory experiments (i.e., permeability test, triaxial test) with core samples from the Ulleung basin. The following equation (Eq. 8) is used to account for the effect of the hydrate saturation on the stiffness of the hydrate-bearing sediment (after Uchida et al. 2012).

$$E_{hydrate} / E_0 = 1 + 13.25 \cdot S_h \tag{1}$$

where $E_{hydrate}$ and $E_0$ are the maximum tangent stiffness of hydrate-bearing soil and non-hydrate soils, respectively.

## 3. UNDERLYING PROCESSES

The coupled mechanical-flow-thermal model using FLAC2D incorporates the physical processes of field-scale methane production in the Ulleung basin. The model mainly includes several assumptions, as follows: (1) the pore fluid flow is governed by Darcy's law, and the hydrate cannot flow; (2) the rate of hydrate dissociation is governed by the first-order kinetics (Kim et al. 1987); (3) the generated methane gas does not flow or dissolve in water; (4) the thermal effect including latent heat, conduction and advection due to pore fluid flowis considered; and (4) the geomechanical response of the hydrate-bearing sediments is in accord with the Mohr-Coulomb model.

Based on the experimental studies (Masuda et al. 1997; Minagawa et al. 2005), the permeability of the hydrate-bearing sediments is found to be a function of the hydrate saturation and the intrinsic permeability of the porous media, as follows:

$$K_h = k_s (1 - S_h)^N \tag{2}$$

where $k_s$ is the intrinsic permeability ($\mathrm{m}^2$) of the sand layer, $S_h$ is the hydrate saturation, and $N$ is a model parameter.

The sediments at the Ulleung basin sites contain fine-grained sediment intercalated with thin sand-rich layers. The modified Kozeny-Carman equation (Bear 1972; Kaviany 1995) is applied to verify the permeability change in the sand layer due to porosity reduction by the effective stress.

$$k_s = f\left(\frac{n^3}{(1-n)^2}\right) = \frac{n^3}{36k(1-n)^2} d^2 \tag{3}$$

where $n$ is the porosity, $k$ is a constant, and $d$ is the mean diameter for the spherical particles. The value of constant $k$ is derived empirically; the mean diameter $d$ is estimated using field coring data. Therefore, the permeability of the hydrate bearing sediments (i.e. the sand layers) can be expressed as a function of the porosity and the hydrate saturation as below.

$$K_h = \frac{n^3}{36k(1-n)^2} d^2 \cdot (1 - S_h)^N \tag{4}$$

Most of the fine-grained sediment samples were classified as highly plastic silty soils;they exhibited high compressibility, high porosity, and low hydraulic conductivity (Kim et al. 2013; Kwon et al. 2011). Considering the results of the consolidation tests with the core samples (Kim et al. 2013), an empirical correlation between the porosity and the permeability of the mud layer was derived, as follows (Fig. 2):

$$k_m = 8 \cdot 10^{-6} \times n^{18.73}, \quad R^2 = 0.8474 \tag{5}$$

where$k_m$ is the intrinsic permeability (m/s) of the mud layer.
It is assumed that no hydrate exists in mud layer as can be seen in Fig. 1. Therefore,it only the porosity changethat has a considerable effect on the permeability.

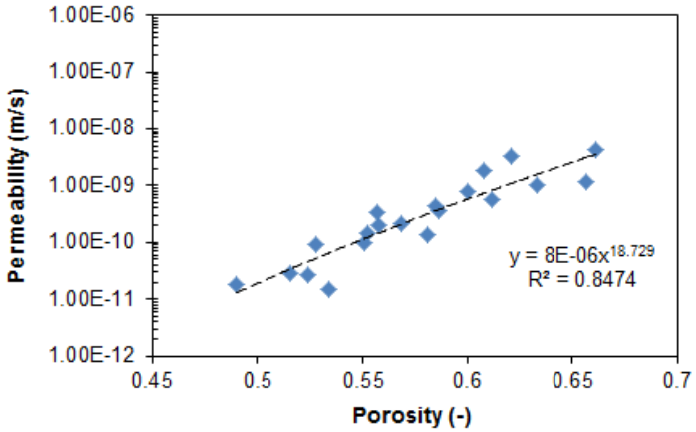


Fig. 2 Empirical correlation between porosity and permeability of mud specimens

## 4. Simulation Results

Fig. 3 shows the porosity change with production time caused by depressurization from the well head. As the effective stress increases due to depressurization, volume contraction of the sediment is generated in the depressurized region. This tendency is more pronounced in the mud layers. In the upper mud layer, there is a large porosity reduction over a larger distance, as indicated by the color difference in Fig. 3. The porosity change spreads to about 30 m after 50 days;the difference in porosity is about 0.05 in the mud layers and about 0.02 in the sand layers. Meanwhile, the lower final bottom hole pressure (BHP) leads to a bigger porosity drop and larger distance of porosity reduction. In the case of the final BHP of 9 MPa, the porosity change spreads to 20-25 m from the well head (after 50 days).

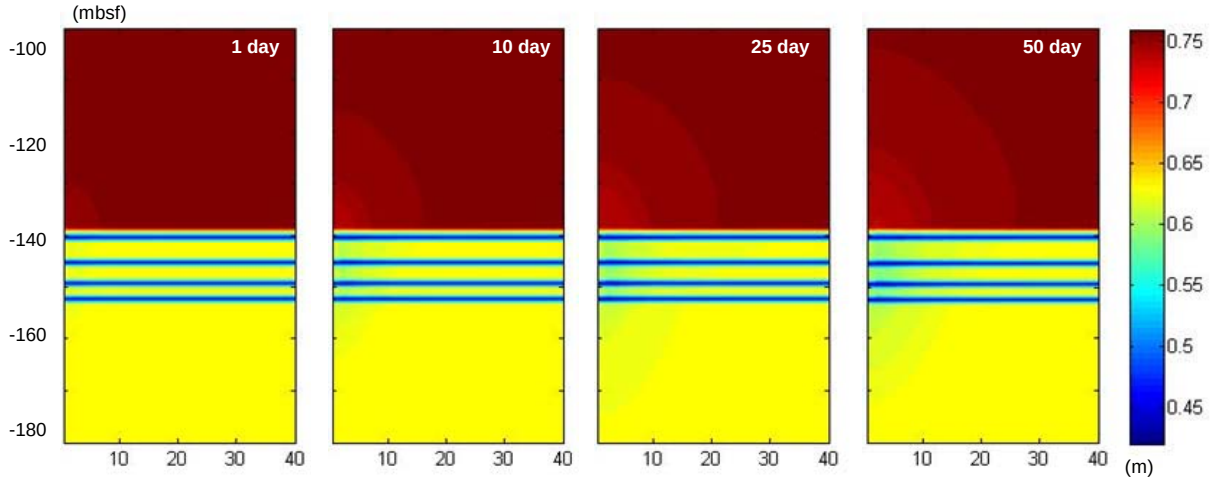


(a) Final bottom hole pressure - 5 MPa

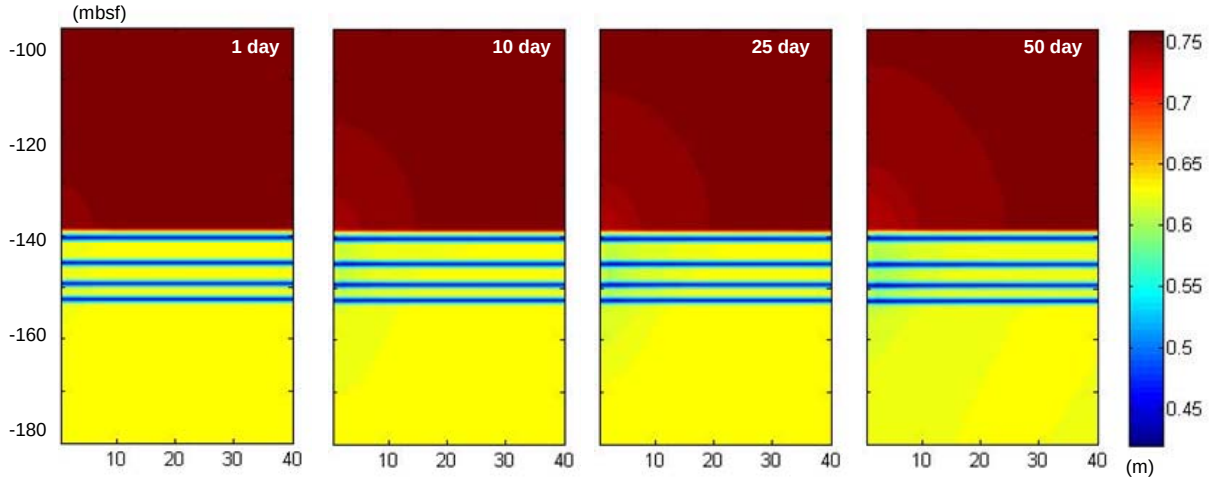


(b) Final bottom hole pressure - 9 MPa

Fig. 3 Spatial distribution of porosity at 1 day, 10 days, 25 days, and 50 days of production period

Fig. 4 shows the spatial distribution of the permeability in the sediments. Owing to the local decrease of the porosity around the well head, the permeability near the well head decreases. As the production time advances, there is a large permeability drop over a larger distance; this distance reaches about 30-40 m after 50 days. In addition, it has been observed that the amount of decrease in the permeability is about half of the initial value, as shown in Fig. 4. Likewise with the results of the porosity change, the difference in permeability according to final BHP is not considerable.

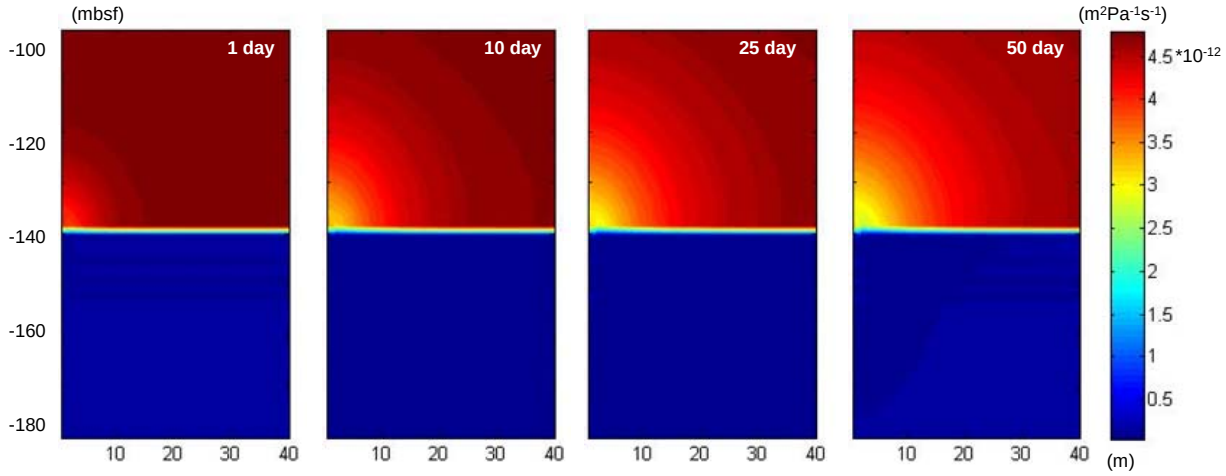


(a) Final bottom hole pressure - 5 MPa

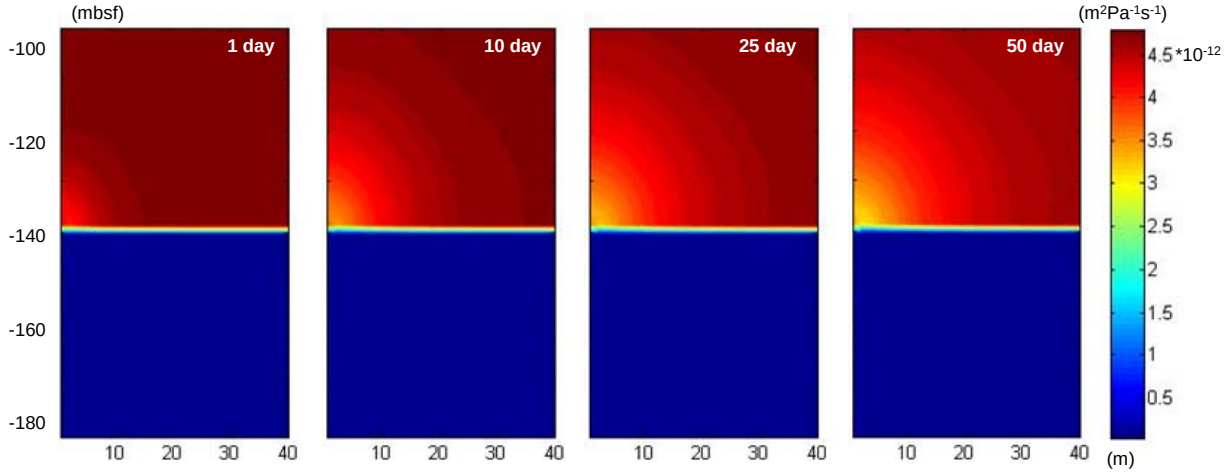


(b) Final bottom hole pressure - 9 MPa

Fig. 4 Spatial distribution of permeability at 1 day, 10 days, 25 days, and 50 days of production period

## 5. CONCLUSIONS

In this study, a field-scale numerical analysis was conducted to explore how porosity reduction affectspermeability in sediments. The geotechnical characteristics and detailed geometry of the Ulleung basin site were considered as input model parameters to simulate *in situ* hydrate production tests. The model includes the physical processes of hydrate dissociation, permeability as a function of hydrate saturation and porosity, and the geomechanical responses of hydrate-bearing sediments. The main findings are that (1) during depressurization, the effective stress increases and volume contraction and porosity reduction of the sediment are thus generated in the depressurized region. According to the empirical correlation derived using the experimental data, a greater decrease in porosity is induced especially at the mud layers. (2) The permeability near the well headalso gradually decreases with porosity reduction, reaching to half the value of the initial intrinsic permeability. This means that the porosity reduction, which

leads to permeability drop in the mud layer, has a considerable effect on the rate and productivity of methane production in theUlleung basin. (3) As a comparative study, two different final BHPswere simulated. The lower final BHP led to larger porosity and permeability drops and spread to a larger distance. However, the overall results for both cases show similar tendencies.

## REFERENCES

Kvenvolden, K.A., and Lorenson, T.D. (2010),"A Global Inventory of Natural Gas Hydrates Occurrence", http://walrus.wr.usgs.gov/globalhydrate.

Milkov, A.V. (2004),"Global estimates of hydrate-bound gas in marine sediments: how much is really out there?"*Earth-Science Reviews*, **66**, 183-197.

Boswell, R., and Collett, T.S. (2011),"Current perspectives on gas hydrate resources",*Energy & environmental science*, **4**(4), 1206-1215.

Moridis, G.J. (2003),"Numerical Studies of Gas Production From Methane Hydrates", *SPE J*., **8**(4), 359-370.

Makogon, Y.F. (1997), "Hydrates of Natural Gas, 1st ed."; Penn Well Publishing Company: Tulsa, USA.

Holder, G.D., Kamath, V.A., and Godbole, S.P. (1984),"The potential of natural gas hydrates as an energy resource",*Annual Review of Energy*, **9**(1), 427-445.

Pawar, R.J., Zyvoloski, G.A., Tenma, N., Sakamoto, Y., and Komai, T. (2005),"Numerical simulation of laboratory experiments on methane hydrate dissociation",*Proc., 15th International Offshore and Polar Engineering Conference*, June, Seoul.

Moridis G.J., and Reagan, M.T. (2007),"Strategies for Gas Production From Oceanic Class 3 Hydrate Accumulations", *Offshore Technology Conference*, 30 April – 3 May, Houston, Texas.

Park, K.P. (2006), "Gas hydrate exploration in Korea",*Proc., 2nd International Symposium on Gas Hydrate Technology*, November, Daejeon, Korea.

Ryu, B.J., Kim, G.Y., Chun, J.H., Bahk, J.J., Lee, J.Y., Kim, J.H., Yoo, D.G., Collett, T.S., Riedel, M., Torres, M.E., Lee, S.R., UBGH2 Scientists.(2012),"The Second Ulleung Basin Gas Hydrate Drilling Expedition (UBGH2) Expedition Report". Korea Institute of Geoscience and Mineral Resources, Daejeon, Korea

Uchida, S., Soga, K., and Yamamoto, K. (2012),"Critical state soil constitutive model for methane hydrate soil",*Journal of Geophysical Research: Solid Earth* (1978–2012), 117(B3).

Kim, H.C., Bishnoi, P.R., Heidemann, R.A. and Rizvi, S.S.H. (1987),"Kinetics of methane hydrate decomposition".*Chemical Engineering Science*, **42**(7), 1645–1653.

Masuda, Y., Naganawa, S., Ando, S., and Sato, K. (1997),"Numerical calculation of gas-production performance from reservoirs containing natural gas hydrates", In Annual Technical Conference, Soc. of Petroleum Eng., San Antonio, Texas, Paper (Vol. 38291).

. Minagawa, H., Ohmura, R., Kamata, Y., Ebinuma, T., Narita, H. and Masuda, Y. (2005),"Water permeability measurements of gas hydrate-bearing sediments",*Proc. 5th International Conference Gas Hydrates*, Trondheim, Norway, 1, 398–401.

. Kim, H.S., Cho, G.C., Lee, J.Y., and Kim, S.J. (2013),“Geotechnical and geophysical properties of deep marine fine-grained sediments recovered during the second Ulleung Basin Gas Hydrate expedition”, East Sea, Korea.*Marine and Petroleum Geology*, 47, 56-65.

Kwon, T.H., Lee, K.R., Cho, G.C., and Lee, J.Y. (2011),“Geotechnical properties of deep oceanic sediments recovered from the hydrate occurrence regions in the Ulleung Basin, East Sea, offshore Korea”,*Marine and Petroleum Geology*, 28, 1870e1883.